J. Earth Syst. Sci. (2024)133 88
https://doi.org/10.1007/s12040-024-02302-6

Magnetic mineral characterization of the easternmost Indus Molasse sedimentary succession, Ladakh Himalaya: Implications for depositional environment and provenance

Mahesh Kapawar[1,*], Subhojit Saha[1], Anil Kumar[1] and Venkateshwarlu Mamilla[2]

[1] *Wadia Institute of Himalayan Geology, 33, GMS Road, Dehradun, India.*
[2] *CSIR-National Geophysical Research Institute, Hyderabad, India.*
[*] *Corresponding author. e-mail: maheshrkapawar@gmail.com*

MS received 28 August 2023; revised 18 December 2023; accepted 27 December 2023

Rock magnetic analyses of easternmost Indus Molasses of Nyoma–Rhongo section, Ladakh Himalaya have been performed. The thermomagnetic curve gives Curie point (Tc) information on the constituent magnetic minerals, which vary between 574° and 592°C. The hysteresis loops are harmonious and the resultant remanence ratio (*Mrs/Ms*) ranges between 0.10 and 0.19 and the coercivity ratio (*Bcr/Bc*) between 1.91 and 3.07. The domain states of magnetic grains majorly belong to the pseudo-single domain (PSD) state. The isothermal remanent magnetization (IRM) acquisition curves show saturation ranges between 250 and 300 mT, and the coercivity spectra show coercive force ranging between 24 and 41 mT. These investigations indicate that magnetic mineralogy in samples is predominantly controlled by fine to medium-sized PSD state magnetite and accessorily Ti-poor magnetite, pyrrhotite, and greigite. This magnetic mineralogy seemed homogenous and was not considerably affected by weathering, lithogenesis and geotectonic events, suggesting their deposition over well-developed palaeogeography with small-scale tectonic modulations. The best possible source for Indus Molasses, as identified in the current study is the Ladakh batholith having an affinity to the Eurasian Plate and these interpretations are in line with the literature.

Keywords. Mineral magnetism; Indus Molasse; sediment provenance; sediment environment; Ladakh batholith.

1. Introduction

The timing and nature of the collision between the Indian and Eurasian plates is a controversial and debated topic in geology (Rowley 1998). Generally, the collision timing is bracketed between 65 and 50 Ma (Cai *et al.* 2011; Searle and Treloar 2019). Although, the timing of the early collision has been constrained between ∼59 Ma to as young as ∼34 Ma (Aitchison *et al.* 2002; Ali and Aitchison 2008) or ∼25 Ma (van Hinsbergen *et al.* 2012; Najman *et al.* 2017). Criteria like cessation of marine facies, the first arrival of the Kohistan–Ladakh arc (KLA) on the Indian Plate, and the relative position of India and Asia with time are relied upon to constrain initial collision (Najman *et al.* 2010). Apart from

Supplementary material pertaining to this article is available on the *Journal of Earth System Science* website (http://www.ias.ac.in/Journals/Journal_of_Earth_System_Science).

Published online: 05 May 2024

collision timing, recent studies have postulated a two-stage collision between the Indian–Eurasian plates. In the first stage, possibly the Indian Plate collided with the KLA along the Indus suture at ∼50 Ma (Khan *et al.* 2009) or at ∼85 Ma (Chatterjee *et al.* 2013). And in the second stage, with the Eurasian Plate along the Shyok suture zone at ∼40–34 Ma. However, the idea of collision in two stages was contested by some workers (Najman *et al.* 2017; Bhattacharya *et al.* 2020) with the argument that both Indus and Shyok sutures were closed by 54 Ma. Though a discrepancy in crustal shortening to the tune of 1000 km may result from the wide variation in collisional timing (van Hinsbergen *et al.* 2012), a general consensus among workers is near ∼3000 km of Neotethyan oceanic crust subducted before the initiation of collision (Rowley 2019; van Hinsbergen *et al.* 2019).

In this backdrop, the molasse (terrestrial) deposits of the Indus Basin along the Indus Suture Zone (ISZ), NW Himalaya, hold orogenic sedimentation records. These records are associated with the uplift and erosion of the southern margin of Asia due to the Indian–Eurasian plates collision since ∼55 Ma. Thick sections of Indus Molasses have been well exposed along the ISZ and are mostly syn- to post-collisional, continental sedimentary rock sequences. These sequences constitute sediments (Searle *et al.* 1990) derived by variable environmental agents such as alluvial fans, fluvial and lacustrine, majorly supplied from the Ladakh batholith and to a minor extent from the Tethyan Himalayas. The literature portrays that Indus Molasses has been studied mostly in light of U–Pb geochronological and isotopic proxies, and very few studies (Yang *et al.* 2015; Ma *et al.* 2016) have taken into account the magnetic proxies. Therefore, to give input for the depositional age of Indus Molasses and also to give onset collision and upliftment information, a detailed paleomagnetic study has been planned. Before that, the samples were subjected to detailed rock magnetic analyses, as shown in the present study. The sole objective of this work is to find out whether Indus Molasse sedimentary rocks sufficiently carry reliable and accurate signals of the geomagnetic field throughout geologic time. As rock magnetic techniques are rapid and non-destructive, they are of great importance for studying the diagenetic and authigenic processes experienced by magnetic minerals of sediments/sedimentary rocks. Magnetic minerals are important for recording sedimentary paleomagnetic signals that are used widely in geosciences (Roberts 2015). Thus, rock magnetic study provides first-order information about the sample's further usefulness in paleomagnetic study to understand the depositional history of Indus Molasses (local) and the upliftment history of the Himalayan mountains (regional) since the Cenozoic.

Therefore, the aim of the present rock magnetic investigations of Indus Molasse sedimentary rocks is to identify the constituent magnetic remanence-carrying minerals, quantify their grain size, detect any kind of digenetic interferences and overall gain knowledge about their suitability for paleomagnetic (magnetostratigraphy) studies. Apart from knowing the sample's suitability for the intended paleomagnetic (magnetostratigraphy) study, the current rock magnetic approach allowed us to comment on the depositional environment and sediment provenance of Indus Molasse.

2. Geological setting

Indus Molasses are syn- to post-collisional sedimentary rocks of ISZ deposited during the Eocene to post-Eocene age. They are products of the collision between the Indian and Eurasian plates, representing a classic example of continent–continent collision. The beginning of molasse sedimentation along the Yarlung Tsangpo Suture Zone (Tibetan part) and the ISZ was regarded as Eocene (Searle *et al.* 1987). In the north of the ISZ lies the Lhasa–Karakoram block (affinity to the Eurasian Plate) and to the south lies the Tethyan Himalaya of northern India. The Indus Molasses covers a considerable part of ISZ in the form of a ∼2000 km long arcuate belt that preserves marine and terrestrial sedimentary records. It is a folded and thrusted sequence of carbonate and clastic formations that unconformably rest over the Ladakh batholith (Clift *et al.* 2002; Wu *et al.* 2007). They are exposed along the southern margin of the trans-Himalayan magmatic arc and extend between Kargil (in the east) and South Tibet through Nyoma–Hanle of eastern Ladakh (Bajpai *et al.* 2004). The Indus Molasse also unconformably overlies the Indian passive margin unit of ophiolitic melanges close to Chilling (Robertson 2000) and south of the Nyoma region near Nidar village. The geological map of the easternmost part of Indus Molasses with sampling locations is depicted (figure 1).

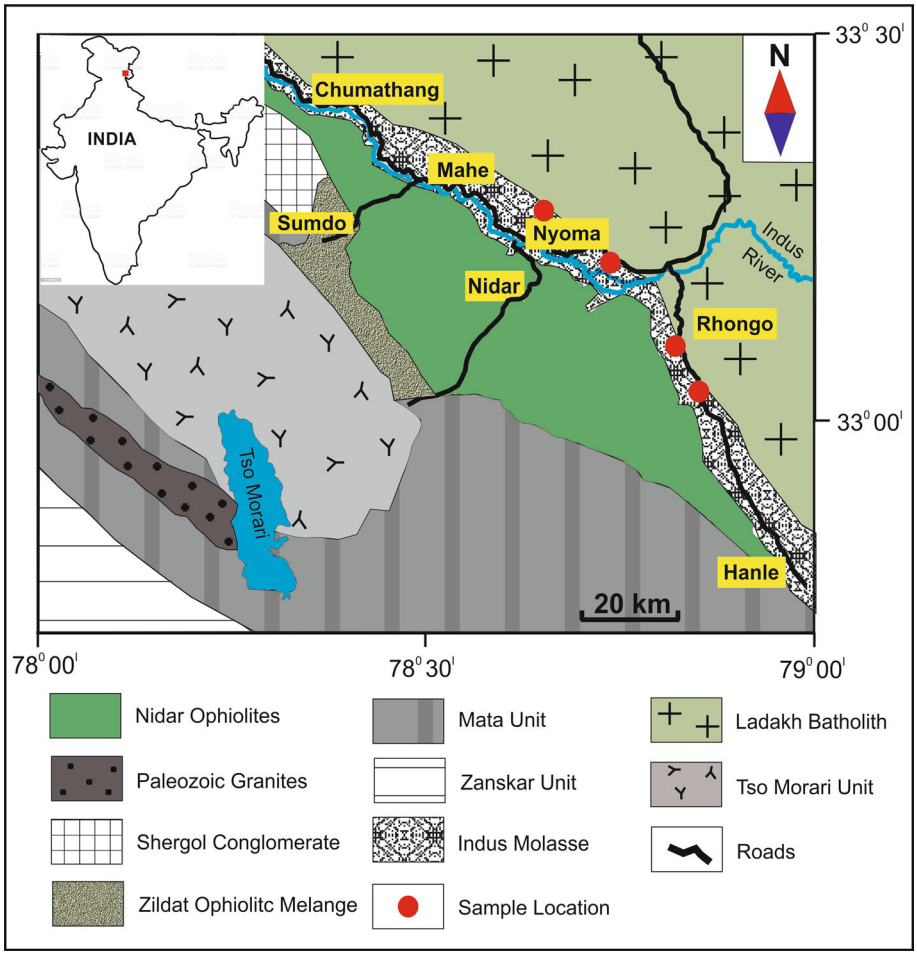

Figure 1. Schematic geological map of part of eastern Ladakh Himalaya constitutes the Indus molassic sedimentary rocks modified after Virdi (1986), Maheo *et al.* (2004) and Bhat *et al.* (2019). The sampling locations are depicted with red circles along the Nyoma–Rhongo transect of the easternmost Indus Molasse.

Indus Molasses are best exposed and studied in the Zanskar Gorge region (Clift *et al.* 2002; Henderson *et al.* 2010), while other exposures further east in eastern Ladakh still need to be addressed and understood. The Indus Molasse (sedimentary rocks of Indus Basin) has been stratigraphically subdivided by different researchers (Garzanti and van Haver 1988; Searle *et al.* 1988, 1990; Sinclair and Jaffey 2001) into two major groups, the older is Tar Group and exposed conformably above this is the younger Indus Group. These groups are subdivided into four distinct formations, each latest by Henderson *et al.* (2010), in an attempt to reassess the stratigraphy of Indus Molasses. Here, the Tar Group has the oldest unit, named Jurutze Formation, overlaid by Sumda and Chogdo formations and the youngest unit of this group is the Nummulitic Limestone Formation, having conformable contact with the older Chogdo Formation. This Nummulitic Limestone Formation of the Tar Group has conformable contact with the base of the Indus Group's Nurla Formation. This Nurla Formation is overlain by the Choksti and Lower Nimu formations. This Lower Nimu Formation has a faulted contact with the Choksti Formation (Searle *et al.* 1990; Sinclair and Jaffey 2001; Clift *et al.* 2002), which was not observed by Henderson *et al.* (2010), and suggested the contact is not conformable. The youngest sedimentary unit of the Indus Group is the Upper Nimu Formation, which is closely juxtaposed south of the Ladakh batholith. The literature studies and our field observations (figure 2) inform us that the lithology of Indus Molasses is majorly controlled by medium to coarse-grained sandstone, carbonates with intraclasts, siltstones, mudstones and partly phyllites. These sediments were mostly deposited in an alluvial fan, fluvial channel, and fluvial floodplain environments (Supplementary figure S1). Apart from this, usual sedimentary structures and features have also been observed. Small-scale extensional faulting and compressional deformations

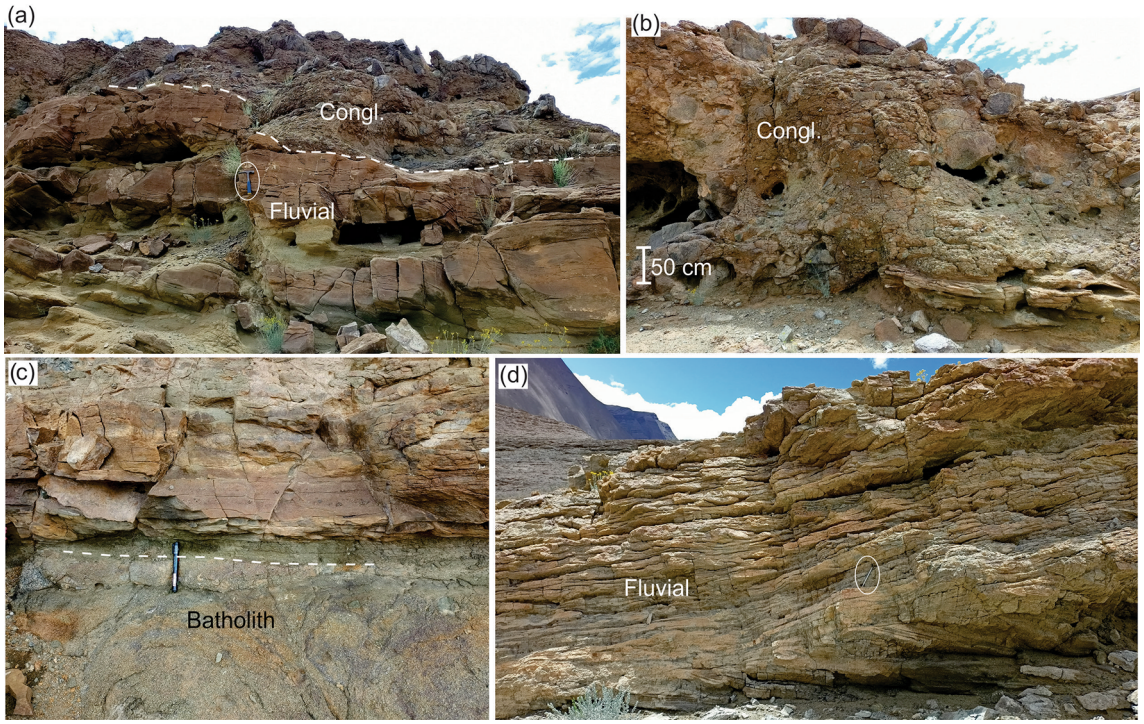

Figure 2. Field photographs from the Nyoma–Rhongo Indus Molasse section. **(a)** The fluvial unit overlain by a thick conglomerate horizon, **(b)** the conglomerate directly overlies the Ladakh batholith, **(c)** fluvial sandstone overlies the Ladakh batholith, and **(d)** the cross-stratified character of the thinly bedded fluvial sandstones.

have been recognized in Indus Molasses (Searle *et al.* 1990; Henderson *et al.* 2010).

3. Sampling and methodology

Indus Molasse sedimentary rock samples were collected from fresh and unweathered outcrops following standard oriented sample collection technique using a Brunton compass and spirit leveller. Sampling was performed along the easternmost Nyoma–Rhongo road section of the ISZ, Ladakh Himalaya (Supplementary table S1). A total of 19 oriented samples from four sites were collected, a minimum of 4–5 oriented rock samples per site. All the collected samples have a distinct separation of around 15–20 m within the site depending on the lithology and freshness of outcrops, thus possessing a good representation of the easternmost part of Indus Molasse. Similar sampling approaches are targeted in the middle and western parts of Indus Molasses to understand magnetic mineralogical variations and eventually carry out rigorous paleomagnetic (magnetostratigraphic) studies.

All the samples were drilled, cut and ground to standard cylindrical specimens (2.5 cm in diameter and 2.2 cm in length) and subjected to bulk magnetic susceptibilities (k) measurements using AGICO's KLY-5A (Czech Republic) susceptibility apparatus at a frequency of 976 Hz, housed at Paleomagnetism Laboratory of Wadia Institute of Himalayan Geology (WIHG), Dehradun. Those samples that yield higher magnetic susceptibility values are then considered for the detailed rock magnetic analyses (two samples/site) since they could sufficiently carry magnetic mineralogical information (Supplementary table S2).

In the laboratory, the petrographic and detailed rock magnetic measurements involving thermomagnetic analysis, magnetic hysteresis loops, acquisition of isothermal remanent magnetization (IRM) and coercivity spectra (backfield demagnetization) have been carried out. Petrographic analyses were carried out on thin sections of the same samples that were used for rock magnetism using a polarising microscope at the Sedimentology Laboratory of WIHG, Dehradun. The rock magnetic measurements were performed in air on powdered samples selected based on magnetic susceptibility measurements. These measurements were carried out using the Advanced Variable Field Translation Balance (AVFTB) instrument at the Paleomagnetism Laboratory of CSIR-National Geophysical Research Institute (NGRI), Hyderabad, India. The rock magnetic data and curves

were visualized using the RockMagAnalyzer software by Leonhardt (2006).

4. Results

A vital aspect in rock magnetic studies is the presence of magnetic remanence carrying minerals in a rock and how the rocks acquire magnetism. This knowledge helps us to consider the rock units to understand the palaeogeography and tectonic evolution of the region. Here, the sample's rock magnetic characteristics were studied to determine the magnetic mineralogy, grain sizes, domain states, and overall magnetic behaviour. We present the detailed rock magnetic results for the first time from the easternmost Indus Molasse sedimentary rocks, Ladakh Himalaya, India.

4.1 *Petrography*

In general, the Indus molassic sandstones are medium to coarse-grained, poorly sorted and arkosic in nature. They are mainly composed of plagioclase, alkali feldspar, biotite, muscovite, quartz, lithic fragments, and opaque grains in minor proportion (figure 3). Plagioclase has been altered to clay and secondary sparry calcite. In some places, euhedral plagioclase exhibits well-developed oscillatory zoning. Biotites are ubiquitous and show evidence of fracturing and deformation. Similarly, orthoclase grains are highly fractured. Quartz shows embayed grain boundary; in rare instances, some bipyramidal quartz has also been observed. The opaque grains present (figure 3) are sparsely distributed in the thin section and could mainly constitute the magnetites.

4.2 *Thermomagnetic curves*

The obtained thermomagnetic curves for the selected samples are shown in figure 4, where the sample's susceptibility in response to increasing temperature is observed. The samples were heated from room temperature to 700°C (heating cycle) and then cooled back to room temperature (cooling cycle). The arrows placed near the heating and cooling cycles (figure 4) suggest the progression of heating and cooling during the experiment. The thermomagnetic curves of samples show the cooling cycles lie below the heating cycles and do not follow each other; they are irreversible indicating that the magnitude of susceptibility is affected by the thermal treatment. Among the analyzed samples, some show single and straight trajectories of the heating cycles that decay around a temperature window of 520–600°C (figures 4A, B, G and H). In other sample's heating cycles (figures 4C, D, E and F) show a distinct decay in susceptibility with increasing temperatures slightly around 320–350°C and majorly around 520–580°C. The thermomagnetic curves of samples IM1.1, IM1.3, IM4.3 and IM4.4 (figures 4A, B, G and H) show straight and steady decay in susceptibility in the heating cycle and yield a single and stable Curie temperature (Tc) of ∼580°C, the cooling cycles follow the heating cycles but with decreased magnitude. This Tc likely corresponds to a stable and predominant ferrimagnetic mineral, magnetite. Samples IM2.4 and IM2.5 (figure 4C and D) display a distinct decrease in susceptibility in the heating cycle, initially around 320°C (Tc1) and then show a major loss in signal at around 520°C (Tc2).

The Tc1 corresponds to the presence of an unstable and weakly magnetized pyrrhotite phase (Dekkers 1989) that alters to a comparatively stable magnetic phase of Ti-poor magnetites (Tc2) regarded as secondary magnetite (of titanomagnetite solid solution series) that adds up to originally existing primary magnetite in samples. Samples IM3.1 and IM3.4 (figure 4E and F) also depicted an initial and gentle fall in susceptibility signal at around 350°C (Tc1) and later steeply decreased around 520°C (Tc2). The Tc1 in this sample could be due to the accessory presence of greigite mineral (Snowball and Thompson 1990; Snowball 1991; Roberts 1995) and later transformed due to heating in a relatively stable magnetic phase of Ti-poor magnetite, again regarded as secondary magnetite. The details about the samples Tc and the associated magnetic mineralogy are provided in table 1. Thermomagnetic curves of the samples are complex but reveal various components responsible for magnetic remanence in samples as indicated by mineralogical transformations during heating cycles (figure 4). Thus, the magnetic mineralogy of Indus Molasses is majorly controlled by magnetite (Tc = ∼585°C), secondarily by Ti-poor magnetites (Tc = ∼520°C), and accessorily by pyrrhotite (Tc = ∼320°C) and greigite (Tc = ∼350°C).

4.3 *Magnetic hysteresis loops*

Magnetic hysteresis loops in the maximum applied magnetic field of 1T were obtained for the selected samples after paramagnetic corrections

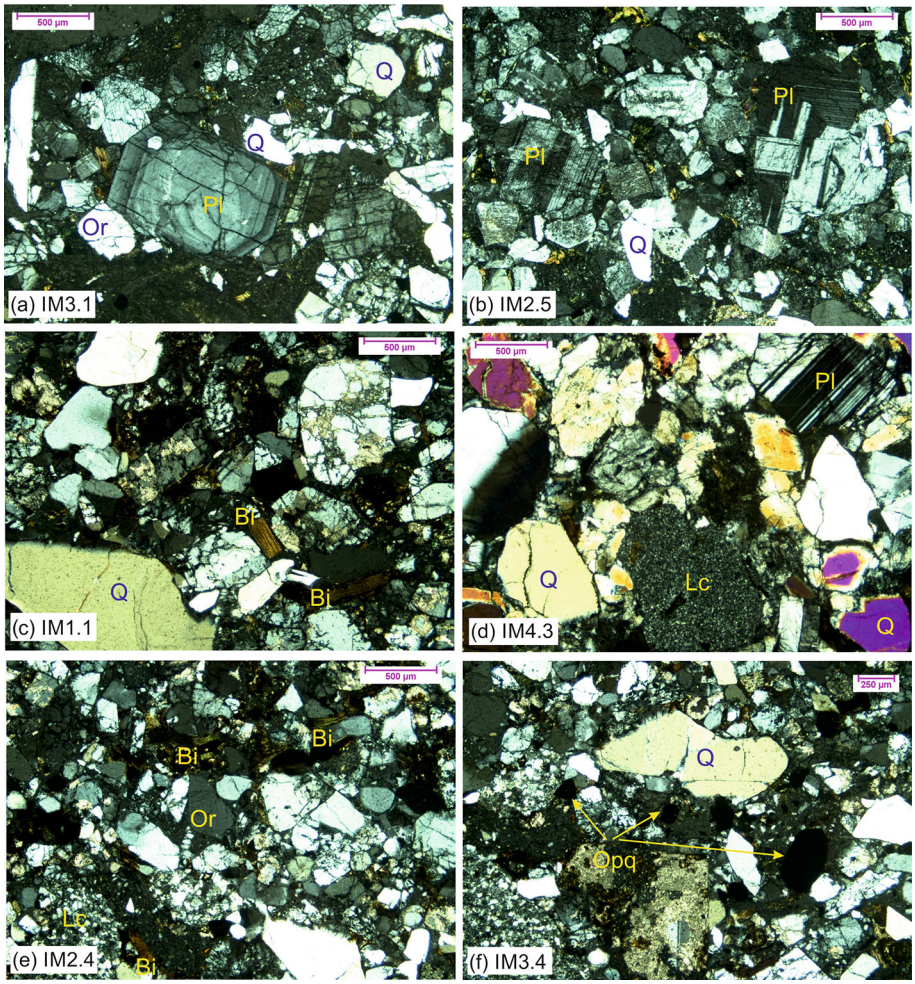

Figure 3. Photomicrographs of Indus Molasse samples showing **(a)** zoned plagioclase, **(b)** dominance of fresh plagioclase feldspar, **(c)** presence of biotite, **(d, e)** presence of lithic clast and **(f)** opaque minerals. Orthoclase: Or, Quartz: Q, Plagioclase: Pl, Biotite: Bi, Lithic clast: Lc, Opaque: Opq.

(figure 5), and details of the hysteresis parameters are provided in table 1. The magnetization saturation for all the samples is visible below 300 mT and the paramagnetic contribution towards susceptibility is negligible, suggesting the susceptibility is mainly governed by ferrimagnetic minerals. All the analyzed samples displayed consistent and identical s-type hysteresis loops in the 'pot-bellied' shape that was thinly closed. Such thin nature of loops may be due to fine to medium-grained magnetic particles. Also, the low coercive magnetic grains in samples govern this shape of loops.

The hysteresis parameters obtained from hysteresis loops were processed and the values of saturation magnetization (*Ms*), saturation remanent magnetization (*Mrs*), coercivity force (*Bc*) and coercivity remanence (*Bcr*) were noted. The schematic Day plot (Day *et al.* 1977) of the remanence ratio (*Mrs/Ms*) against the coercivity ratio (*Bcr/Bc*) has been developed to obtain information about the domain state of magnetic minerals and thus their average grain size (figure 6). The present study samples have a *Mrs/Ms* ratio ranging from 0.10 to 0.19 and a *Bcr/Bc* ratio ranging from 1.91 to 3.07. The Day plot distinguishes the single domain (SD), pseudo-single domain (PSD), and multidomain (MD) magnetic grains and thus serves as a better measure of the magnetic mineral's grain size.

The Day plot results reveal that most of the magnetic remanence carriers have grain size falls within the PSD region, possibly due to an admixture of SD and MD particles. Thus, the magnetic grain size can be revealed to be fine to medium-sized. The hysteresis properties of the present study samples are majorly commanded by the stable and fine-grained magnetic phase of magnetite and the influence of accessory phases seems negligible.

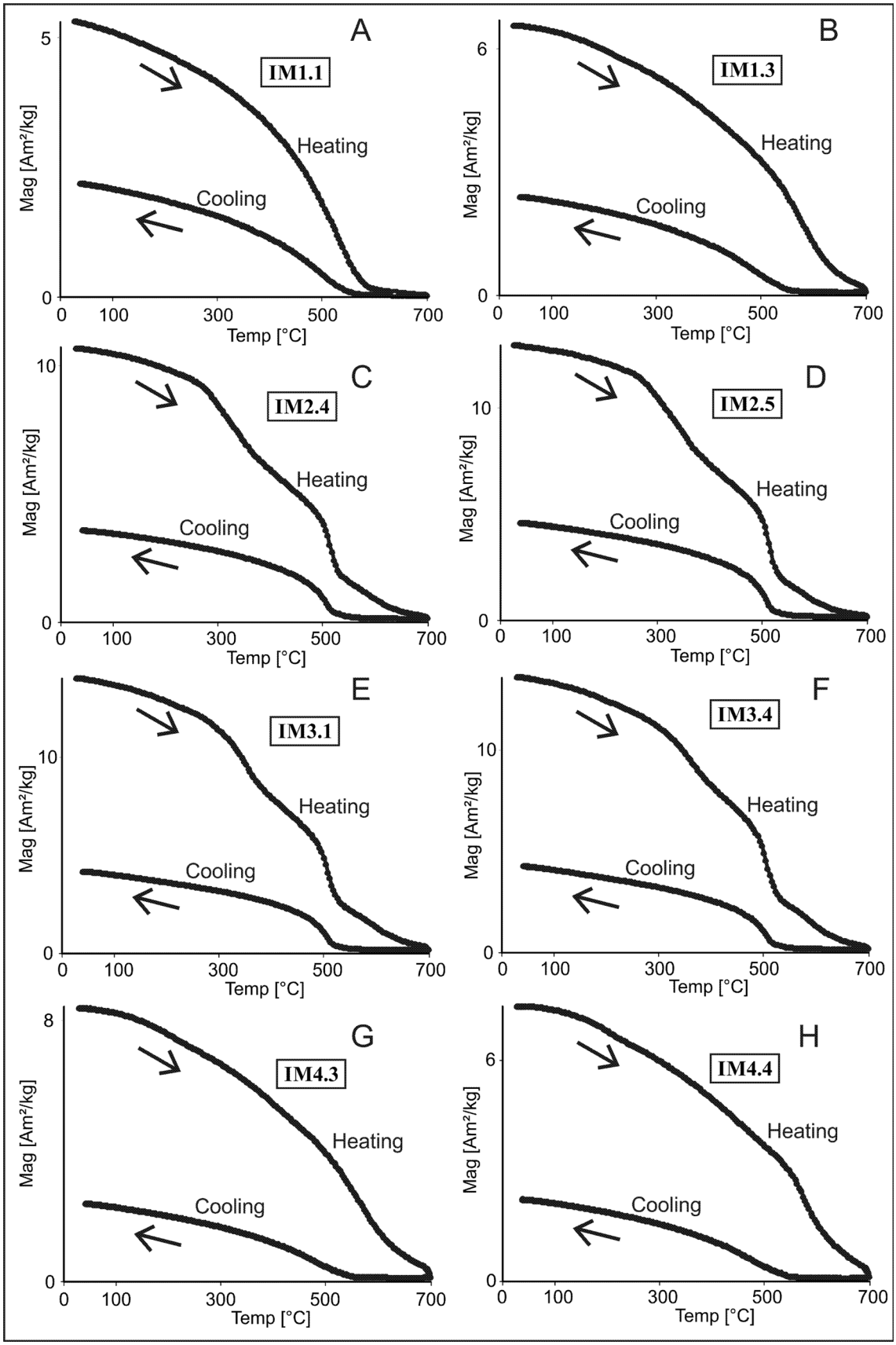

Figure 4. Thermomagnetic (magnetic susceptibility, k *vs.* temperature, T) curves for samples. Arrows show the progression of heating (heating cycle) from room temperature to a maximum of 700°C and back to room temperature (cooling cycle). Sample numbers are shown in the boxes.

Table 1. *The detailed rock magnetic characteristics of representative Indus Molasse samples.*

Sample ID	*Mrs* (Am^2/kg)	*Ms* (Am^2/kg)	*Mrs/Ms*	*Bcr* (mT)	*Bc* (mT)	*Bcr/Bc*	Tc (°C)	Magnetic mineralogy
IM1.1	2.36	12.0	0.19	31.13	16.29	1.91	574	Magnetite
IM1.3	2.17	19.4	0.11	34.94	12.37	2.82	592	Magnetite
IM2.4	3.93	28.0	0.14	42.96	15.37	2.79	521, 317	Magnetite (Ti-poor magnetite), Pyrrhotite
IM2.5	4.54	33.4	0.13	42.20	14.50	2.91	520, 327	Magnetite (Ti-poor magnetite), Pyrrhotite
IM3.1	4.86	37.0	0.13	39.92	13.92	2.86	522, 352	Magnetite (Ti-poor magnetite), Greigite
IM3.4	4.67	35.9	0.13	39.63	13.90	2.85	521, 355	Magnetite (Ti-poor magnetite), Greigite
IM4.3	2.66	25.4	0.10	37.71	12.25	3.07	588	Magnetite
IM4.4	2.33	22.2	0.10	36.94	12.13	3.04	580	Magnetite

Note: Mrs = Saturation remanent magnetization; *Ms* = Saturation magnetization; *Bcr* = Coercivity remanence; *Bc* = Coercive force; Tc = Curie Temperature in degree Celsius.

4.4 *IRM acquisition curves and coercivity spectra*

Magnetic mineralogy is a mixture of differential magnetization saturation levels with high and low coercivity mineral phases. The acquisition of IRM and the coercive force primarily gives knowledge of magnetic mineralogy. Here, samples were subjected to these analyses to modify and/or strengthen the outcomes of the above rock magnetic measurements.

The IRM-acquisition curves of the samples and their respective coercivity spectra are shown (figure 7), indicating the IRM signal went up at the beginning in response to the applied magnetic field. About 90% of the IRM curves have attained saturation by a field of 300 mT in most of the samples, which suggests the presence of low coercive magnetic minerals. These coercivity spectra (figure 7) support the contention that low coercive magnetic minerals are present, since the coercivity values are below 50 mT in all the samples. It is thus speculated that these samples contain soft magnetic minerals as the main magnetic remanence carriers. The elementary conclusion that can be drawn from IRM and coercivity analyses is that samples have saturated to 90% by 300 mT in IRM, and coercivity values below 50 mT are due to the predominance of soft and less coercive magnetic minerals like magnetite.

5. Discussion

5.1 *Inferred magnetic mineralogy*

The magnetic mineralogy associated with the sedimentary rocks of Indus Molasse is mainly attributed to ferrimagnetic magnetites (primary and secondary) and Ti-poor magnetites (belongs to a titanomagnetite solid solution series). These minerals not only have a dominant presence in samples but also have an association with other unstable and poorly present iron sulfides (pyrrhotite and greigite). The thermomagnetic curves are irreversible and indicate that pyrrhotite and greigite underwent thermal alteration during heating and were later transformed into magnetite (secondary) completely and added up to the primary magnetite. This neoformation of magnetite (secondary) during the heating cycles is variable with high thermal stability. The thermomagnetic curves of samples depict no secondary peak during

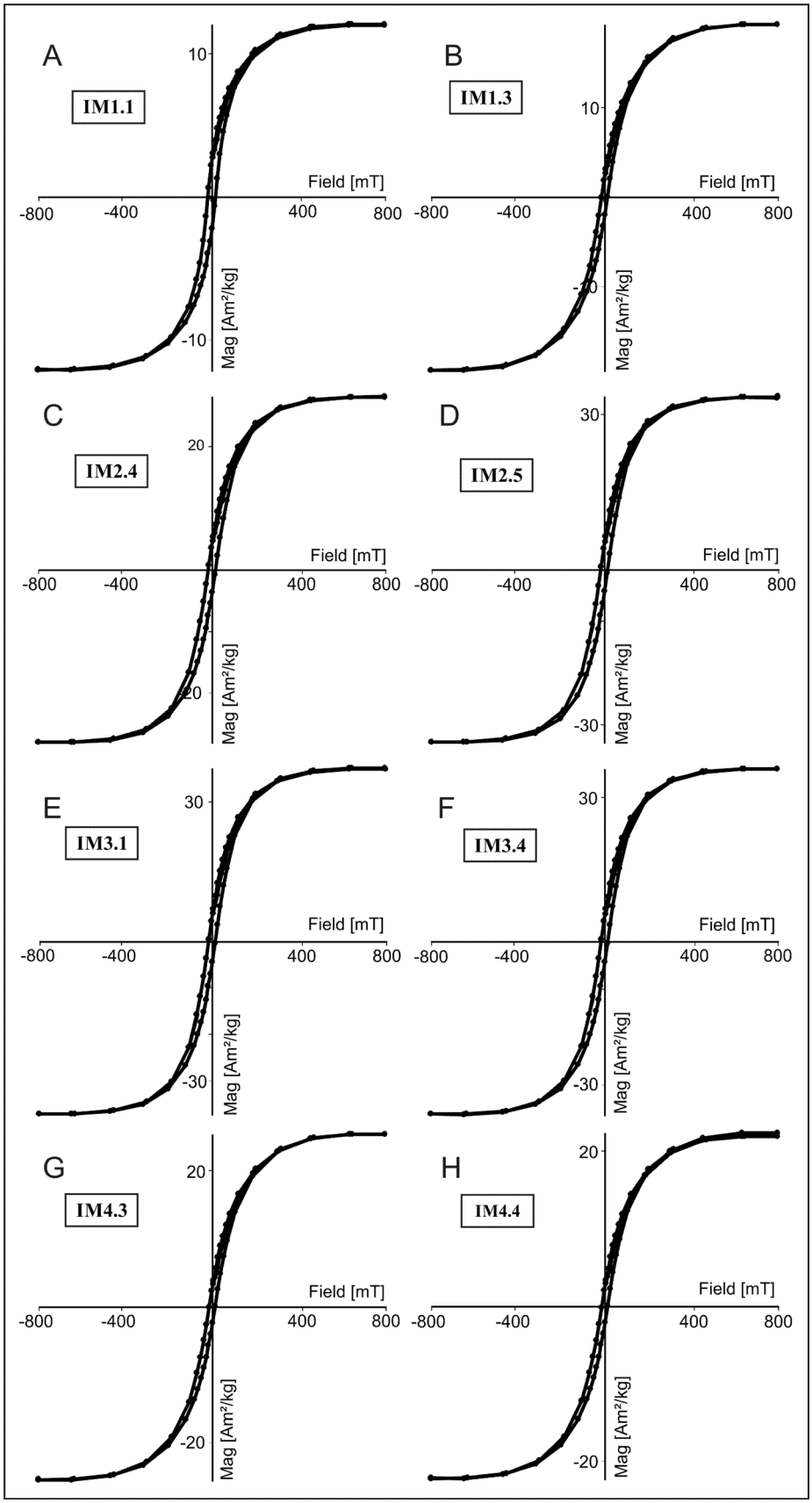

Figure 5. Hysteresis loops of typical pot-bellied shape for the samples of Indus Molasses. The hysteresis loops are after the paramagnetic corrections. Sample numbers are shown in the boxes.

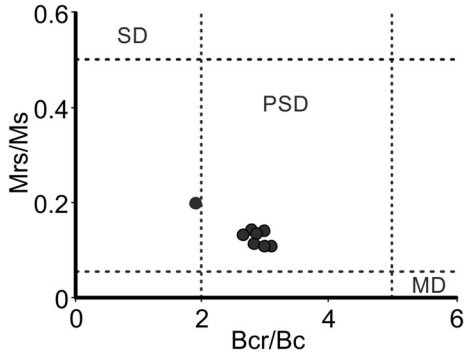

Figure 6. The bivariate Day diagram for Indus Molasses: SD, PSD and MD are single-domain, pseudo-single domain, and multidomain fields for magnetic grains, respectively. The black circles represent samples that majorly belong to the PSD state. *Mrs/Ms* and *Bcr/Bc* ratios were calculated after the paramagnetic correction.

the cooling cycle, which evidences magnetite's sole predominance in the samples.

Pyrrhotite exhibits minimal presence in samples, identified by blunt loss of susceptibility in the heating curve around 310–330°C (which is Tc of pyrrhotite) in samples IM2.4 and IM2.5 (figure 4), which later completely transformed to a stable magnetic mineral phase. The first report of pyrrhotite in the Himalayas as the secondary remanence carrier was from the Manang area of Nepal (Appel *et al.* 1991) and later by Appel *et al.* (1995), Rochette *et al.* (1994), Schill *et al.* (2001), etc., in other parts of the Himalaya. These studies are in line with the current study results of pyrrhotite occurrence in the Himalaya and their decomposition into a newer and more stable magnetic phase of ferrimagnetic magnetite (secondary).

Another accessory magnetic mineral present in samples is greigite, an authigenic ferrimagnetic mineral associated with early digenesis of the sedimentary rock. A relatively small change in susceptibility in a heating cycle is observed at ∼350°C, after which susceptibility majorly dropped at ∼520°C. This indicates the presence of a relatively small and unstable amount of greigite (IM3.1, IM3.4; figure 4) that decomposed to Ti-poor magnetites. The greigite gets completely decomposed in response to increased heating; hence, the cooling cycle shows only the presence of Ti-poor magnetite in samples (figure 4; Frank *et al.* 2007). Several proposed pathways for the greigite mineral formation require the content of sulfide and iron available at the time of diagenesis (Roberts and Weaver 2005). The presence of pyrrhotite and greigite in samples preserves magnetic remanence records that were acquired during final deposition/lithification and thus reliably renders the geomagnetic field variations (if any).

The dissolution and neoformation of magnetite (i.e., the secondary magnetite) have been identified in the current study, confirmed by the absence of pyrrhotite and greigite in the cooling cycles of thermomagnetic curves. The hysteresis parameters revealed that the pyrrhotite and greigite bearing samples show PSD behaviour, and the neoformed Ti-poor magnetites and magnetites also behaved similarly, i.e., falling in the PSD range. A remarkable work with magnetites was done by Dunlop (1995), who suggested that most magnetite grains that carry paleomagnetic remanence fall in the PSD range. Analogous to this, the dominance of PSD magnetite in the current study and their rock magnetic characteristics suggests that Indus Molasses carry sufficient magnetic remanence. Thus making them suitable for paleomagnetic and geotectonic-related studies (regional tectonics, structural geology, geodynamics, etc.). The obtained domain states of magnetic minerals using a Day plot are valid for pure (Ti-) magnetite bearing samples only, and no or poor contribution of accessory minerals (here pyrrhotite and greigite) is recorded.

5.2 *Grain size effects and depositional environment*

There are visible correlations between the particle size of sedimentary rocks and grain size of constituent magnetic minerals (Oldfield 1994; Zhang *et al.* 2001). The variations in magnetic properties usually are due to the differential grain size of magnetic minerals. The Indus Molasses has stable and consistent mineral magnetic characteristics. Hence, grain-size dependency is limited. Samples have fine- to medium-sized magnetic grains and are majorly dominated by the PSD state of magnetite. This implies not much variation in magnetic grain size and thus, sediment input to the ISZ is constrained from the local origin. Small seasonal streams and slope erosion could be the major agents of sediment supply for, at least, the easternmost part of the Indus Molasse. Stable and consistent magnetic mineralogy with observed sedimentary structures upholds the idea of ISZ marking the exact line of collision between the Indian and Eurasian plates.

The magnetite is chemically adequately strong during the sediment transport to survive, although

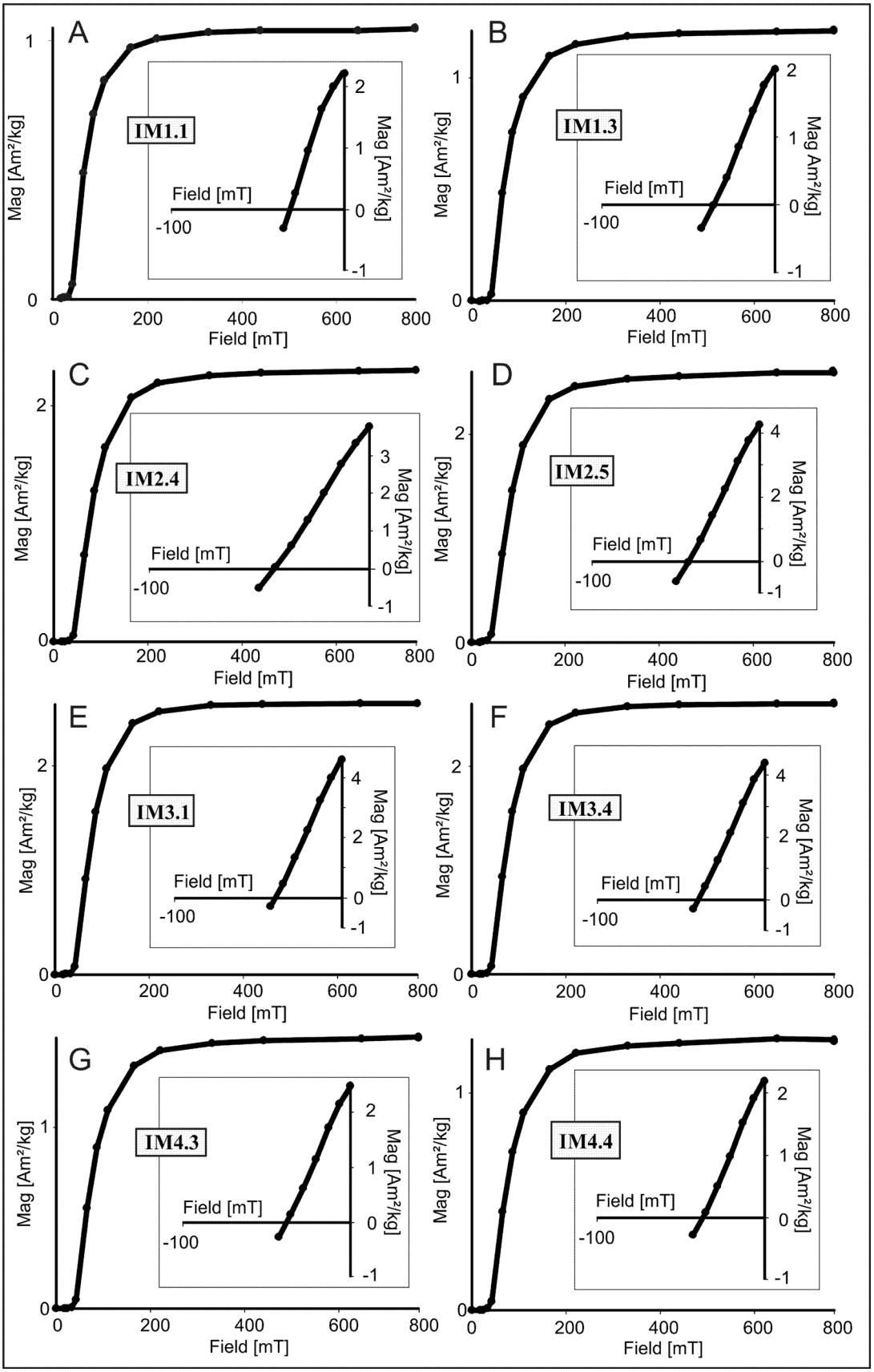

Figure 7. IRM acquisition curves and in the inset are their respective coercivity curves (backfield IRM). Sample numbers are shown in the boxes.

these particles experience some superficial oxidization. The substitute occurrence of iron sulfides (greigite and pyrrhotite) in Indus Molasses indicates that the sediments transportation was less and the possible source area is nearer, which is also supported by petrographic evidence. The study area (easternmost Indus Molasse) was tectonically least active, and no major tectonic uplift and/or subsidence were experienced during their deposition and lithification. These interpretations are in accord with the results of Searle *et al.* (1990) and Aitchison *et al.* (2007), who suggested a tectonically quiescent period after the initial phase of thrusting between the Indian–Eurasian plates around the early Eocene.

Changes in magnetic parameters in sedimentary rocks can be caused by several factors, some of which can be attributed to the sediment depositional environment. Since the variations in rock magnetic properties of the studied samples are very less thus informs stable, consistent, and faster sedimentation. Uniform grain size and stable magnetic properties may further indicate a relatively steady sediment supply in the easternmost Indus Molasse basin. For extending the knowledge gained from the current study which is greatly based on rock magnetic characteristics, a detailed magnetostratigraphic approach is required. This will further permit to comment on the rate of sedimentation since the early to mid-Cenozoic times. Such an attempt will also allow detailed insight into the lithostratigraphic evolution of the Indus basin, Ladakh Himalaya.

In the photomicrographs (figure 3), the opaque grains are identified as magnetite grains of euhedral to subhedral textures and occur alongside other magnetic minerals (pyrrhotite and greigite). As a whole petrographic observations support the rock magnetic results.

5.3 *Sediment provenance*

With the India–Eurasia collision during ∼50–55 Ma, the intense reworking of pre-existing lithology brought down the material to the Indus basin and may offer knowledge of the thermal evolution of the ISZ. The occurrence of pre-collisional marine sediments in ISZ (Searle *et al.* 1990) marks their paleo-Tethyan affinity.

One of the several sediment provenance methods is an examination of rock magnetic properties, which helps identify the sediment-source relation. In the present study, the resultant rock magnetic properties are consistent, it appears that this part of Indus Molasses (easternmost Indus Molasses) has been relatively stable and less possibly affected by any tectonic activity. Here, the magnetic mineralogy is dominantly governed by magnetites (primary = already existing in the rocks and secondary = neoformed by decomposition of unstable magnetic minerals) and accessorily carried by magnetic minerals such as greigite and pyrrhotite (iron sulfides). The lack of variations in rock magnetic properties is associated with quick sediment deposition in the easternmost part. The inferred magnetic minerals showed the effects of some chemical changes due to heat, which resulted in a small range of mineralogical transformations/alterations that slightly affected the magnetic mineral assemblages of the Indus Molasses. These slight changes may be associated with weak remagnetization (secondary magnetization) imposed in them with time by small-scale diagenesis (Lowrie and Heller 1982; Karlin and Levi 1983).

The magnetic mineralogy shows consistent rock magnetic characters and the occurrence of greigite (authigenic mineral) in samples, indicating that the sediment source for the easternmost part of the Indus Molasses is local. The north-lying Ladakh batholith is best possibly the source of detrital material since it falls close to the Indus Molasse basin. The sediments derived from such a close vicinity were less transported, deposited, finally lithified, and turned into sedimentary rock units of Indus Molasse. Early syn-collisional sediments were feasibly deposited directly upon an uplifted and eroded surface that developed over the Ladakh batholith (south of the Eurasian Plate); these sediments were entirely derived from the north, with the Ladakh arc and Karakoram terrane being the most likely sources (Zhou *et al.* 2020).

The nature of the Indus molassic rocks has been well examined by researchers (e.g., Garzanti *et al.* 1987; Searle *et al.* 1990; Clift *et al.* 2002; Henderson *et al.* 2010) and suggested two sources (1) Indian passive margin and (2) Ladakh batholith. The present study results agree with the literature work of Kumar (2008) on the magnetite series of granites in Ladakh batholiths, suggesting that the Indus molassic sediments were dominantly sourced from the Eurasian margin, i.e., Ladakh batholith. Also, the current study results are in agreement with the literature work of Sangode *et al.* (2013), suggesting the sediment inputs to the Leh Valley basin of the

Indus River were from the near-source region. Similarly, Trivedi *et al.* (1982) reported the accessory presence of the magnetite and titanomagnetite in Gaik granites of Ladakh batholiths, thus satisfactorily supporting our contention of genetic link between Indus Molasse and Ladakh batholiths. Rather at present no direct confirmable indications of Indus Molasses's Eurasian affinity (Ladakh batholiths) are available, and inputs from the Indian Plate cannot be denied. To examine this possibility, more robust work on similar lines to the present study should be conducted from other parts of the Indus Molasses and rocks of Ladakh batholiths.

Two ferrimagnetic iron sulfides (pyrrhotite and greigite) that are important to paleomagnetism analyses can carry substantial magnetization signals, and both are present in the Indus Molasse samples. Pyrrhotite and greigite are important minerals to consider when evaluating sedimentary basin's thermal history (Akatakpo and Geissman 2022) like the Indus Molasse basin. The pyrrhotite in samples is locally attributed to the degradation of the pre-existing rock, in which the high temperature and stable ferrimagnetic phase get accumulated, i.e., magnetite. Likewise, greigite is an authigenic sedimentary mineral that forms during sediment accumulation by precipitation or recrystallization of pre-existing lithology. Such a significant occurrence of pyrrhotite and greigite with dominant magnetite in the mineral assemblage is indicative of the preservation of stable paleomagnetic directions (Kars and Kodama 2015; Roberts 2015; Yang *et al.* 2022) and may also be useful for strength estimations of the geomagnetic field (paleointensity). Eventually, we demonstrate that these easternmost Indus molassic sedimentary rocks preserve reliable records of the geomagnetic field and thus are suitable for paleomagnetic (magnetostratigraphy) and paleointensity studies.

6. Conclusions

We investigated the rock magnetic properties of samples from the easternmost Nyoma–Rhongo transect of Indus Molasse, Ladakh Himalaya. The results of thermomagnetic measurements indicate that the dominant magnetic mineral is magnetite with a range of Tc between 574 and 592°C. The hysteresis measurements indicate that samples mostly exhibit a pseudo-single domain (PSD) state of magnetic minerals with fine to medium grain size. The IRM acquisition curves approach to saturation by ∼300 mT, with coercivity values below 50 mT, confirms the magnetic minerals in samples are soft and low-coercive. This predominant, high thermal stability and low-coercive magnetic mineral is regarded as magnetite (and Ti-poor magnetite), and other accessory magnetic minerals present are pyrrhotite and greigite (iron sulfides). Consistent and stable rock magnetic results in the present study indicate that the sedimentary rocks of the Indus Molasse might have lithified over well-developed palaeogeography with minor post-lithification variations.

The Indian–Eurasian plates collision is a global event of geoscientific interest that seems wrongly attributed to the widely accepted time (∼50–55 Ma), but the on-site collision appears to have lagged ∼20 Ma (Aitchison *et al.* 2007), thus proposing a requirement of critical paleogeographic reassessment. To solve this discrepancy in the exact timing of collision, an attempt at a paleomagnetic (magnetostratigraphy) study in combination with a detailed geological mapping could be vital. The present study validates the usefulness of Indus Molasses for the paleomagnetic (magnetostratigraphy) study.

We finally remark that the ambient environment that existed during the formation of Indus Molasse was likely stable with small-scale tectonic modulations (localized, i.e., in the easternmost part of Indus Molasse in ISZ) within the large-scale deformational regime (regional, i.e., Himalayan Orogeny).

Acknowledgements

The authors are grateful to the Director of Wadia Institute of Himalayan Geology, Dehradun, for the necessary grant for fieldwork and permission to publish this work (WIHG/0299). The Director of CSIR-National Geophysical Research Institute, Hyderabad, is thanked for the permission to use the Paleomagnetism Laboratory facility. We express our gratitude to the Associate Editor, Dr Joydip Mukhopadhyay, for carefully handling the paper. Also, we are indebted to Dr H Wabo and an anonymous reviewer whose comments and suggestions substantially improved this paper.

Author statement

Mahesh Kapawar: Conceptualization, methodology, formal analysis, investigation, data curation,

validation, writing – original draft, review and editing. Subhojit Saha: Methodology, formal analysis, investigation, writing – review and editing. Anil Kumar: Methodology, formal analysis, writing – review and editing. Venkateshwarlu Mamilla: Methodology, formal analysis, writing – review and editing.

References

Aitchison J C, Davis A M and Luo H 2002 New constraints on the India–Asia collision: The lower Miocene Gangrinboche conglomerates, Yarlung Tsangpo suture zone, SE Tibet; *J. Asian Earth Sci.* **21** 253–265.

Aitchison J C, Ali J R and Davis A M 2007 When and where did India and Asia collide?; *J. Geophys. Res.* **112** B05423, https://doi.org/10.1029/2006JB004706.

Akatakpo S O and Geissman J W 2022 Paleomagnetism and rock magnetism of Permian sedimentary rocks and Early Jurassic Karoo (Large Igneous Province) sills intersected in the KWV-1 borecore, Eastern Cape Province, South Africa; *J. Afr. Earth Sci.* **194** 104627, https://doi.org/10.1016/j.jafrearsci.2022.104627.

Ali J R and Aitchison J C 2008 Gondwana to Asia: Plate tectonics, paleogeography and the biological connectivity of the Indian subcontinent from the Middle Jurassic through latest Eocene (166–35 Ma); *Earth Sci. Rev.* **88** 145–166, https://doi.org/10.1016/J.EARSCIREV.2008.01.007.

Appel E, Muller R and Widder R W 1991 Palaeomagnetic results from the Tibetan Sedimentary Series of the Manang area (north central Nepal); *Geophys. J. Int.* **104** 255–266.

Appel E, Patzelt A and Chouker C 1995 Secondary palaeoremanence of Tethyan sediments from the Zanskar range (NW-Himalaya); *Geophys. J. Int.* **122** 227–242.

Bajpai S, Whatley R C, Prasad G V R and Whittaker J E 2004 An Oligocene non-marine ostracod fauna from the Basgo Formation (Ladakh Molasse), NW Himalaya, India; *J. Micropalaeont.* **23** 3–9.

Bhat I M, Ahmad T and Subba Rao D V 2019 Origin and evolution of Suru Valley Ophiolite peridotite slice along Indus suture zone, Ladakh Himalaya, India: Implications on melt-rock interaction in a subduction-zone environment; *Geochemistry* **79** 78–93, https://doi.org/10.1016/j.chemer.2018.10.003.

Bhattacharya G, Robinson D M and Wielicki M M 2020 Detrital zircon provenance of the Indus Group, Ladakh, NW India: Implications for the timing of the India–Asia collision and other syn-orogenic processes; *Geol. Soc. Am. Bull.* **133** 1007–1020.

Cai F L, Ding L and Yue Y 2011 Provenance analysis of upper Cretaceous strata in the Tethys Himalaya, southern Tibet: Implications for timing of India–Asia collision; *Earth Planet. Sci. Lett.* **304(3–4)** 356–368.

Chatterjee S, Goswami A and Scotese C R 2013 The longest voyage: Tectonic, magmatic, and paleoclimatic evolution of the Indian plate during its northward flight from Gondwana to Asia; *Gond. Res.* **23** 238–267.

Clift P D, Carter A, Krol M and Kirby E 2002 Constraints on India–Eurasia collision in the Arabian sea region taken from the Indus Group, Ladakh Himalaya, India. The tectonic and climatic evolution of the Arabian Sea region; *Geol. Soc. London, Spec. Publ.* **195** 97–116.

Day R, Fuller M and Schmidt V A 1977 Hysteresis properties of titanomagnetites: Grain-size and compositional dependence; *Phys. Earth Planet. Int.* **13(4)** 260–267.

Dekkers M J 1989 Magnetic properties of natural pyrrhotite. II. High and low temperature behaviors of Jrs and TRM as a function of grain size; *Phys. Earth Planet. Int.* **57** 266–283.

Dunlop D J 1995 Simulation of magnetic hysteresis in pseudo-single-domain grains of magnetite; *J. Geophys. Res.* **100(B3)** 3859–3871.

Frank U, Nowaczyk N R and Negendank J F W 2007 Rock magnetism of greigite bearing sediments from the Dead Sea, Israel; *Geophys. J. Int.* **168** 921–934, https://doi.org/10.1111/j.1365-246X.2006.03273.x.

Garzanti E and Van Haver T 1988 The Indus clastics: Fore-arc basin sedimentation in the Ladakh Himalaya (India); *Sedim. Geol.* **59(3–4)** 237–249, https://doi.org/10.1016/0037-0738(88)90078-4.

Garzanti E, Baud A and Mascle G 1987 Sedimentary record of the Northward Flight of India and its collision with Eurasia (Ladakh Himalaya, India); *Geodin. Acta* **1(4–5)** 297–312.

Henderson A L, Najman Y, Parrish R, BouDagher-Fadel M, Barford D, Garzanti E and Andò S 2010 Geology of the Cenozoic Indus Basin sedimentary rocks: Paleoenvironmental interpretation of sedimentation from the western Himalaya during the early phases of India–Eurasia collision; *Tectonics* **29** TC6015, https://doi.org/10.1029/2009TC002651.

Karlin R and Levi S 1983 Diagenesis of magnetic minerals in recent haemipelagic sediments; *Nature* **303** 327–330.

Kars M and Kodama K 2015 Authigenesis of magnetic minerals in gas hydrate-bearing sediments in the Nankai Trough, offshore Japan; *Geochem. Geophys. Geosyst.* **16(3)** 947–961, https://doi.org/10.1002/2014GC005614.

Khan S D, Walker D J, Hall S A, Burke K C, Shah M T and Stockli L 2009 Did the Kohistan-Ladakh Island arc collide first with India?; *Geol. Soc. Am. Bull.* **121(3–4)** 366–384.

Kumar S 2008 Magnetic susceptibility mapping of Ladakh granitoids, northwest higher Himalaya: Implication to redox series of felsic magmatism in the subduction environments; *Geol. Soc. India Memoir* **72** 83–102.

Leonhardt R 2006 Analyzing rock magnetic measurements: The RockMagAnalyzer 1.0 software; *Comput. Geosci.* **32** 1420–1431, https://doi.org/10.1016/j.cageo.2006.01.006.

Lowrie W and Heller F 1982 Magnetic properties of marine limestones; *Rev. Geophys.* **20(2)** 171–192.

Ma Y, Yang T, Bian W, Jin J, Zhang S, Wu H and Li H 2016 Early Cretaceous paleomagnetic and geochronologic results from the Tethyan Himalaya: Insights into the Neotethyan paleogeography and the India–Asia collision; *Sci. Rep.* **6(1)** 21605.

Maheo G, Bertrand H, Guillot S, Villa I M, Keller F and Capiez P 2004 The South Ladakh ophiolites (NW Himalaya, India): An intra-oceanic tholeiitic arc origin with implication for the closure of the Neo-Tethys; *Chem. Geol.* **203** 273–303.

Najman Y, Appel E, Fadel M B, Bown P, Carter A, Garzanti E, Godin L, Han J, Liebke U, Oliver G, Parrish R and Vezzoli G 2010 Timing of India–Asia collision: Geological,

biostratigraphic, and palaeomagnetic constraints; *J. Geophys. Res.* **115(B12416)** 1–18.

Najman Y, Jenks D, Godin L, Boudagher-Fadel M, Millar I, Garzanti E, Horstwood M and Bracciali L 2017 The Tethyan Himalayan detrital record shows that India–Asia terminal collision occurred by 54 Ma in the Western Himalaya; *Earth Planet. Sci. Lett.* **459** 301–310.

Oldfield F 1994 Toward the discrimination of fine-grained ferrimagnets by magnetic measurements in lake and near-shore marine sediments; *J. Geophys. Res.* **99** 9045–9050.

Roberts A P 1995 Magnetic properties of sedimentary greigite (Fe_3S_4); *Earth Planet Sci. Lett.* **134** 227–236.

Roberts A P 2015 Magnetic mineral diagenesis; *Earth Sci. Rev.* **151** 1–47, https://doi.org/10.1016/j.earscirev.2015.09.010.

Roberts A P and Weaver R 2005 Multiple mechanisms of remagnetization involving sedimentary greigite (Fe_3S_4); *Earth Planet Sci. Lett.* **231** 263–277, https://doi.org/10.1016/j.epsl.2004.11.024.

Robertson A H F 2000 Formation of melanges in the Indus Suture Zone, Ladakh Himalaya by successive subduction-related, collisional and post-collisional processes during Late Mesozoic-Late Tertiary time; In: *Tectonics of the Nanga Parbat Syntaxis and the Western Himalaya* (eds) Khan M A, Treloar P J, Searle M P and Qasim M, *Geol. Soc. London, Spec. Publ.* **170** 333–374.

Rochette P, Scaillet B, Guillot S, LeFort P and Pecher A 1994 Magnetic properties of the High Himalayan leucogranites: Structural implications; *Earth Planet. Sci. Lett.* **126** 214–234.

Rowley D B 1998 Minimum age of initiation of collision between India and Asia north of Everest based on the subsidence history of the Zhepure Mountain section; *J. Geol.* **106** 229–235.

Rowley D B 2019 Comparing paleomagnetic study means with apparent wander paths: A case study and paleomagnetic test of the Greater India versus Greater Indian Basin hypotheses; *Tectonics* **38** 722–740, https://doi.org/10.1029/2017TC004802.

Sangode S J, Rawat S, Meshram D C, Phadtare N R and Suresh N 2013 Integrated mineral magnetic and lithologic studies to delineate dynamic modes of depositional conditions in the Leh valley basin, Ladakh Himalaya, India; *J. Geol. Soc. India* **82** 107–120, https://doi.org/10.1007/s12594-013-0129-0.

Schill E, Appel E, Zeh O, Singh V K and Gautam P 2001 Coupling of late-orogenic tectonics and secondary pyrrhotite remanences: Towards a separation of different rotation processes and quantification of rotational underthrusting in the western Himalaya (N-India); *Tectonophys.* **337** 1–21.

Searle M P and Treloar P J 2019 Introduction to Himalayan tectonics: A modern synthesis; *Geol. Soc. London, Spec. Publ.* **483** 1–17.

Searle M P, Windley B F, Coward M P, Cooper D J W, Rex A J, Rex D, Tingdong L, Xuchang X, Jan M Q, Thakur V C and Kumar S 1987 The closing of Tethys and the tectonics of the Himalaya; *Geol. Soc. Am. Bull.* **98(6)** 678–701.

Searle M P, Cooper D J W and Rex A J 1988 Collision tectonics of the Ladakh–Zanskar Himalaya; *Philos. Trans. Roy. Soc. London, Ser. A* **326** 117–150.

Searle M P, Pickering K T and Cooper D J W 1990 Restoration and evolution of the intermontane Indus Molasse basin, Ladakh Himalaya, India; *Tectonophys.* **174(34)** 301–314, https://doi.org/10.1016/0040-1951(90)90327-5.

Sinclair H D and Jaffey N 2001 Sedimentology of the Indus group, Ladakh, northern India: Implications for the timing of initiation of the palaeo-Indus River; *J. Geol. Soc. London* **158** 151–162, https://doi.org/10.1144/jgs.158.1.151.

Snowball I 1991 Magnetic hysteresis properties of greigite (Fe_3S_4) and a new occurrence in Holocene sediments from Swedish Lappland; *Phys. Earth Planet. Int.* **68** 32–40.

Snowball I and Thompson R 1990 A stable chemical remanence in Holocene sediments; *J. Geophys. Res.* **95** 4471–4479.

Trivedi J R, Gopalan K, Kisharma K, Gupta K R and Choubey V M 1982 Rb−Sr age of Gaik granite, Ladakh batholith, northwest Himalaya; *Proc. Indian Acad. Sci.* **91** 65–73, https://doi.org/10.1007/BF03028028.

Van Hinsbergen D J J, Lippert P C, Dupont-Nivet G, McQuarrie N, Doubrovine P V, Spakman W and Torsvik T H 2012 Greater India Basin hypothesis and a two-stage Cenozoic collision between India and Asia; *Proc. Natl. Acad. Sci.* **109** 7659–7664.

Van Hinsbergen D J J, Lippert P C, Li S, Huang W, Advokaat E L and Spakman W 2019 Reconstructing Greater India: Paleogeographic, kinematic, and geodynamic perspectives; *Tectonophys.* **760** 69–94.

Virdi N S 1986 Indus–Tsangpo suture in the Himalaya: Crustal expression of a palaeo-subduction zone; *Ann. Soc. Geol. Pol.* **56** 3–31.

Wu F Y, Clift P D and Yang J H 2007 Zircon Hf isotopic constraints on the sources of the Indus Molasse, Ladakh Himalaya, India; *Tectonics* **26** TC2014, https://doi.org/10.1029/2006TC002051.

Yang T, Ma Y, Bian W, Jin J, Zhang S, Wu H, Li H, Yang Z and Ding J 2015 Paleomagnetic results from the Early Cretaceous Lakang Formation lavas: Constraints on the paleolatitude of the Tethyan Himalaya and the India–Asia collision; *Earth Planet. Sci. Lett.* **428** 120–133.

Yang T, Dekkers M J, Zhao X, Petronotis K E and Chou Y M 2022 Greigite formation modulated by turbidites and bioturbation in deep-sea sediments offshore Sumatra; *J. Geophys. Res.* **127** e2022JB024734, https://doi.org/10.1029/2022JB024734.

Zhang W G, Yu L Z and Hutchinson S M 2001 Diagenesis of magnetic minerals in the intertidal sediments of the Yangtze Estuary, China and its environmental significance; *Sci. Total Environ.* **266** 169–175, https://doi.org/10.1016/S0048-9697(00)00735-X.

Zhou R, Aitchison J C, Lokho K, Sobel E R, Feng Y and Zhao J X 2020 Unroofing the Ladakh Batholith: Constraints from autochthonous molasse of the Indus Basin, NW Himalaya; *J. Geol. Soc.* **177** 818–825, https://doi.org/10.1144/jgs2019-188.

Corresponding editor: Joydip Mukhopadhyay